Universitat de les Illes Balears

MASTER'S THESIS

SEAGRASS SPATIOTEMPORAL DYNAMICS WITH A TIME-DEPENDENT MORTALITY

Jorge Mampel Danta

Master's Degree in Physics of Complex Systems

Centre for Postgraduate Studies

Academic Year 2021-22

SEAGRASS SPATIOTEMPORAL DYNAMICS WITH A TIME-DEPENDENT MORTALITY

Jorge Mampel Danta

Master's Thesis

Centre for Postgraduate Studies

University of the Balearic Islands

Academic Year 2021-22

Key words:

Seagrass, Posidonia Oceanica, Non-linear, spatiotemporal, Climate change, Modelling

Thesis Supervisor's Name Damià Gomila Villalonga, Daniel Ruiz Reynés

Agraïments

A Damià i Dani per la seua inestimable ajuda i guia.

A totes les persones que m'han acompanyat enguany, en especial les companyes del màster, la companyia de teatre de la UIB i la Maitaldea.

A Ali, Edu i ma mare per creure en mi més que jo mateix.

A totes les persones que lluiten per la nostra terra i el nostre mar.
També a les víctimes, humanes i no-humanes, de l'avarícia i meninfotisme d'eixa minoria amb tant poder.

Resum

La *Posidonia Oceanica* és una part vital dels ecosistemes costaners del Mediterrani, amb efectes positius des de proveir aliments i recer a altres organismes marins a previndre l'erosió de les costes i mitigar el canvi climàtic. L'activitat humana està danyant aquestes praderies mil·lenàries a un ritme alarmant, en part degut al canvi climàtic, ja que l'increment de temperatura de l'aigua augmenta la mortalitat d'aquesta planta marina. L'objectiu d'aquest treball és estudiar els possibles canvis en les dinàmiques espaciotemporals de la *P. Oceanica*, centrant-nos en l'efecte d'una mortalitat dependent del temps.

Com volem investigar els efectes de l'heterogeneïtat espacials i els efectes col·lectius de la *P. Oceanica*, farem servir un model que incloga aquests factors. El model emprat inclou termes espacials i no linears arran de tindre en compte interacciones col·lectives i no locals, i captura fenòmens complexos com la formació de patrons, biestabilitat i punts de no retorn. Dos escenaris teòrics s'estudiaran: Un increment lineal amb el temps de la mortalitat i un increment abrupte d'aquesta. Al primer cas, un llindar en el ritme d'increment de la mortalitat s'ha trobat per damunt del qual els patrons no es poden formar i aleshores la vida d'una praderia cau ràpidament, ja que aquest mecanisme de resiliència es perd. Quan la mortalitat es canvia abruptament, un arrelentiment crític s'observa i, per mortalitats just damunt el punt de no retorn, regions de la praderia desapareixen independentment unes de les altres. En general, queda de manifest la importància de tindre en compte l'estrucutra i dinàmica espacial per a comprendre completament la situació i evolució de la praderia. S'ha tractat de fer prediccions de l'evolució de les praderies a causa de l'escalfament global basant-se en dades de camp. Tot i que les incerteses a les dades dificulta la presentació de conclusions quantitatives firmes, les ferramentes emprades per a estudiar aquestes dades incorporant una major part de la complexitat d'aquestes praderies s'ha explorat, servint com un pas endavant en l'enteniment del destí de les praderies de *P. Oceanica*.

Abstract

Posidonia Oceanica is a vital part of the Mediterranean coastal ecosystem, with positive effects ranging from providing food and shelter to other marine organisms to preventing coastal erosion and mitigating climate change. Human activity is damaging these millenary meadows at an alarming rate, partly through climate change, since water warming increases this seagrass' mortality. The aim of this work is to study the possible changes in the spatiotemporal dynamics of *P. Oceanica*, focusing on the effect of a time-dependent mortality.

Since we want to investigate the effects of spatial heterogeneity and collective effects, we will use a model that accounts for these factors. The model used includes spatial and non-linear terms accounting for collective and non-local interactions, and it captures complex phenomena such as pattern formation, bi-stability and tipping points. Two theoretical scenarios will be studied: A linear increase of mortality with time and an abrupt increase of mortality. In the first case, a threshold in the mortality increase rate is found over which patterns are not formed and hence the lifespan of a meadow decreases abruptly since this mechanism of resilience is lost. When the mortality is changed abruptly, critical slowing down is observed and, for mortalities just above the tipping point, patches of meadow disappear independently of each other. In general, the importance of taking the spatial structure and dynamics into account to fully understand the situation and evolution of a meadow is made clear. An attempt to make predictions of the evolution of meadows with an increase of mortality due to global warming based on field data is made. Although uncertainties in the data and the model hinder the capacity of presenting firm quantitative conclusions, the tools to study this data incorporating more of the meadow's complexity is explored, serving as a step forward in the understanding of the fate of *P. Oceanica* meadows.

Contents

1 Introduction

Posidonia Oceanica is a seagrass endemic of the Mediterranean Sea and a key part of its coastal ecosystems. This clonal plant forms extensive meadows that set the foundations of the trophic network as the main producer and provide shelter to many organisms. It can be found at depths starting at 0.3m and, in very clear waters such that enough light can reach it, up to 45m. An estimated 50 000 km^2 of seafloor, around 3% of the Mediterranean basin, is occupied by it [1]. Its ribbon-like leaves grow vertically with a typical height of 1m and cause the meadows to have a noticeable impact on the hydrodynamics of coastal currents and be efficient particle and floating sediment filters [2].

P. Oceanica, and seagrass in general, are among the main carbon sinks in the biosphere, with a *P. Oceanica* patch having an estimated carbon absorption capacity 15 times larger than an equally sized patch of rainforest [3]. The high rate at which organic matter is produced from CO_2 is complemented by low nutrient and oxygen concentration in the meadow's sediments, so organic matter decomposes slowly, allowing a large part to be buried indefinitely under the meadow, raising the seafloor[4]. If a meadow is lost, there is a risk of this organic matter being released into the sea where it can eventually release the trapped carbon back into the atmosphere.

Whilst individual shoots may live around 30 years, meadows can persist for millennia. In fact, a massive P. Oceanica meadow on the Ibizan coast contends for the title of the longest-lived organism in existence to have been discovered, with estimates of its age having a lower bound of 12 000 years and upper bounds of up to 200 000 years [5]. This extraordinarily long life is one of the reasons why meadows are such large carbon sinks, with depths of up to 11m of buried carbon having been documented under millenary meadows [6].

1.1 Spatial structure of meadows

In spring, seeds are released and drift for several days before sinking and trying to hold on to the seabed and form a new plant, but this has a very low rate of success. The main method of propagation of *P. Oceanica* meadows is clonal growth, with rhizomes that slowly extend horizontally (at a parsimonious rate of around 5 cm y^{-1}) and sprout vertical shoots at roughly regular intervals, such that shoots are regularly separated by a typical distance. Whilst some meadows are fairly homogeneous at a landscape scale, others have been found to show diverse heterogeneous patterns even in otherwise homogeneous environments.

These types of patterns are found in other vegetation landscapes, marine and terrestrial, and serve to reorganise the pathways of energy and resources in some conditions [7]. These conditions are generally those of scarcity of resources or large stress on the ecosystem, making it incapable of supporting a dense homogeneous meadow. These patterns can be observed through satellite images in shallow waters (under 5m) and through sonar cartography for deeper waters. Using these tools, the project LIFE Posidonia [8] provides a set of maps of the seafloor in several regions of the Balearic coast. In some cases, like in the neighbouring bays of Pollença and Alcúdia, the spatial structure is quite complex, as can be seen in Figure 1. The main het-

erogeneous pattern seen is of meadow with holes, but smaller regions show regular patches of meadow over bare sand, and channels or stripes. In all these cases, the patterns show a degree of regularity in size and spacing of their features larger than what one would find in a disordered structure.

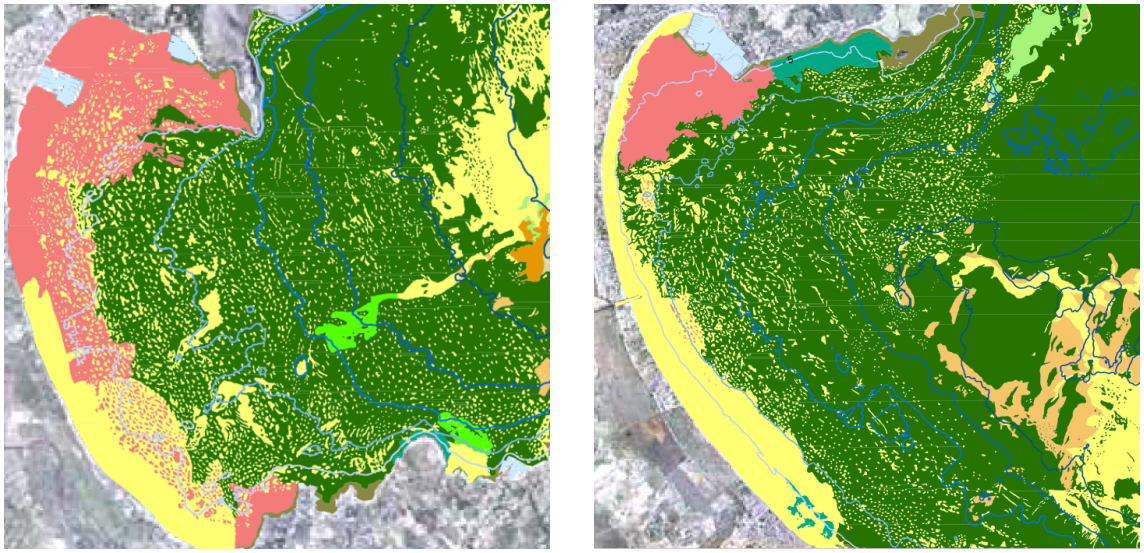

Figure 1: Segrass meadow cartography of the bays of Pollença (a) and Alcúdia (b) at the north of Mallorca [8]. The green regions correspond to *P. Oceanica* meadows, the pink to mixed communities of the seagrass *C. Nodosa* and the algae *Caulerpa Prolifera*, and yellow to sand.

1.2 Monitoring and protection

Due to the ecological importance of *P. Oceanica*, efforts have been made to monitor its situation. By analysing all available works studying the extent and density of meadows since 1842 [9], a decline in the density and extension of these meadows has been documented in many regions where it grows. Several key factors have been attributed to it: physical aggressions such as those from fishing or docking yachts, nutrient imbalances from runoff fertilisers or waste, an increase in water turbidity and coastal works, amongst others.

Estimates of the areal extent decrease of seagrasses in the Mediterranean basin in 50 years (from 1959 to 2009) are in the range of 13% to 50% . The remaining meadows have seen their density halved in 20 years, on average, and become more fragmented. Due to the slow speed of expansion, the losses are hard to recover from: If a region of meadow is lost, the best the meadow can do is expand horizontally 5 cm each year to repopulate the lost region.
The possibilities of restoration and protection projects to mitigate the damages caused and plant new shoots have been studied and some projects are already being developed [10, 11, 12]. If done correctly, these can prevent existing meadows from disappearing and accelerate meadow expansion beyond what would be naturally possible with slow clonal growth.

1.3 Effects of temperature rise

The effects of water temperature on mortality have also been studied, both by studying field data [13, 14] and performing studies in a controlled laboratory environment [15]. Both methods give evidence of the detrimental effects of high temperature on seagrass growth.

The laboratory study [15] consisted of planting a single shoot in water and substrate conditions replicating that found in their natural environment. After a period of acclimatisation, different samples were exposed to different water temperatures and their vertical growth rates measured. The results for all different macrophytes studied were a bell-type curve for growth against temperature (Figure 2a). For *P. Oceanica*, the maximum growth rate was attained for $\sim 27°C$ and the growth rate dropped below 0 for $\sim 33°C$.

In the field study [13], parcels in several meadows in the natural park of Cabrera were delineated and the number of shoots measured yearly. From the change in density from one year to another, the rate of loss, or mortality, of the meadow within said parcel was calculated. The maximum Seawater Surface Temperature ($\mathrm{SST}_{\mathrm{max}}$) for each year was also measured at each site. From these two measurements, the dependence of mortality on temperature was studied, as can be seen for a single site in Figure 2b, where the shoot density was plotted against that year's the corresponding $\mathrm{SST}_{\mathrm{max}}$. In all cases, the drastic increase in $\mathrm{SST}_{\mathrm{max}}$ from 2002 to 2003 gave rise to a decrease in density of up to 40%. A general trend of decreasing density with increasing $\mathrm{SST}_{\mathrm{max}}$ was observed. These results show the negative effect of high temperatures on meadows, especially understood as a mass mortality event when the temperature crosses a threshold of around 28°C, as stated in the article itself as a main conclusion.

Quantitative predictions of the decline of meadows due to temperature increase were later made using these results, predicting the year of extinction (density dropping below 10% of the present density) of the meadows they studied to be 2061 ± 13 by combining the aforementioned field measurements with predictions of seawater temperature rise according to climate models [16]. Something that differentiates global warming from the other anthropogenic causes mentioned earlier is that it can cause losses even in meadows isolated from direct human impact, as was the case in the studied meadows. Also, whilst some impacts, such as physical aggressions, can be quickly stopped, this is not the case with global warming.

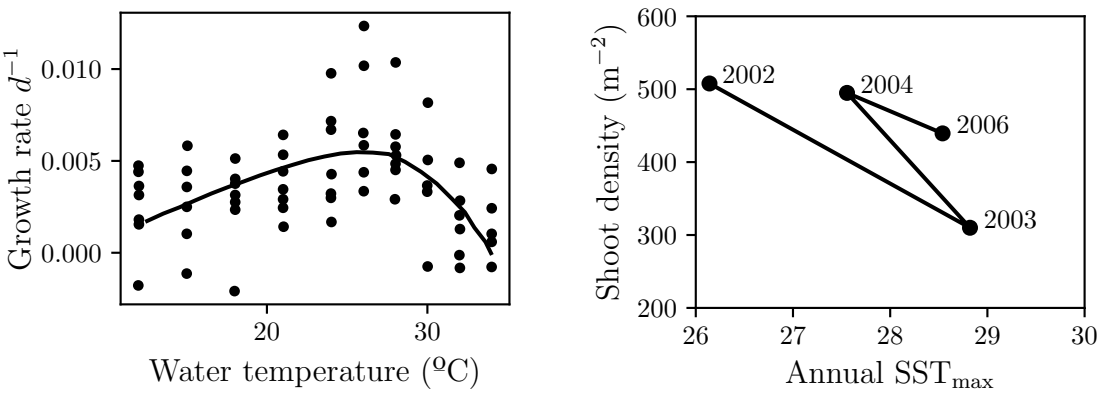

Figure 2: Results from studies of the effect of water temperature on *P. Oceanica* growth rates. Panel (a) the effect of water temperature on vertical leave growth in laboratory conditions [15]. Points correspond to individual samples, and the line to the fit made. Panel (b) shows the shoot density in terms of the $\mathrm{SST}_{\mathrm{max}}$ for an observation parcel in a *P. Oceanica* meadow in the natural park of Cabrera [13]

.

1.4 Modelling

In both cited studies regarding the effects of temperature, non-linear and collective phenomena were left out, either by the experimental design in the laboratory case, where isolated shoots were studied or in the mathematical assumptions for the population dynamics in the field study. The collective effects due to interactions amongst shoots, which can be both facilitative and competitive were thus not taken into account. These effects depend on density, which varied considerably throughout the sites studied due to depths being different: densities of up to 700 shoots m^{-2} were registered at 5m depth and as low as 140 shoots m^{-2} at 25m depth.

There is now a good theoretical [17, 18, 19] and empirical understanding of pattern formation in terrestrial (often arid) ecosystems [20, 21], where the interactions amongst the plants give rise to complex regular patterns. These interactions are often mediated by competition for water or other resources, creating a distribution that maximises the overall density for the available resources whilst distributing the meadows spatially in a way that these resources are not depleted at any particular point. In the case of underwater meadows, lack of water is evidently not a driving mechanism, but competition for other resources such as sunlight, CO_2 or space can play a similar role [22, 23]. Positive interactions also exist, like the dampening of strong waves and currents or sediment trapping [24]. Over time, the meadows are expected to evolve in a way that minimises competition and maximises facilitation. In the particular case of clonal plants such as *P. Oceanica*, spatial interactions are especially important compared to isotropic seed diffusion[25].

By studying the growth mechanisms of *P. Oceanica*, one can derive a microscopic description [26, 27], that is, modelling all individual shoots and rhizomes. Whilst this is ideal from the precision point of view, working with the positions and interactions of individual shoots can be quite cumbersome for medium-sized meadows and analytical studies of the equations will be harder to perform. For large enough

meadows (relative to shoot spacing), a coarse-grained model (in terms of continuous density – not individual shoots) can be derived to describe the spatiotemporal evolution of a meadow. One such model is the ABD (Advection, Branching Death) model [28], which preserves a strong link to the biological observables but offers a continuous approach and can be better analysed analytically. It consists of a pair of integro-differential equations with an explicit angular dependence, making the model effectively three-dimensional. The non-local interactions are introduced via a kernel $\mathcal{K}(\vec{r}-\vec{r}')$ that weights the intensity and sign of the interaction between two positions. This is the hardest term to connect with real measurements since the exact interaction mechanisms are still not fully understood.

Further approximations can be made to reduce this to a single PDE, referred to as the Clonal Growth Model [25]. This exchanges the explicitly long-range terms of the ABD model for an effectively local model, but keeps the dynamical regimes and the saddle-node bifurcation they both present at the same mortality value. Whilst some quantitative correction is lost with these approximations, a simpler model will allow us to better explore the possible scenarios relevant to a changing mortality scenario, both numerically and analytically.

2 Clonal growth model

The clonal growth model [25], which will be used throughout the thesis, consists of the following PDE:

$$\partial_t n = -\omega n + an^2 - bn^3 + \varepsilon\nabla^2 n + \alpha(\nabla^2 n)n + \delta|\vec{\nabla} n|^2 + \beta(\nabla^4 n)n, \tag{1}$$

where n is the shoot density and is space-dependent, $n = n(\vec{x}, t)$. The intrinsic mortality ω will be the control parameter and accounts for the rate at which shoots die (shoot mortality ω_{d0}) and the rate at which new shoots are recruited due to rhizomes branching (branching rate ω_b): $\omega = \omega_{d0} - \omega_d$. This is equivalent to the mortality in a linear model, in the sense that, if the spatial and non-linear effects were somehow eliminated, for example, isolating a single shoot.
The other parameters will be taken as constants and have the following interpretations:

an^2 : Facilitative interactions that allow meadows to exist for positive mortalities.

$-bn^3$: Saturation, being small for small densities but growing fast for larger values until the total growth rate is 0 and the maximum density is attained.

$\varepsilon\nabla^2 n$: Effective diffusive term due to clonal growth and branching.

$\left.\begin{matrix}\alpha(\nabla^2 n)n \\ \beta(\nabla^4 n)n\end{matrix}\right\}$: Long range interactions between plants.

$\delta|\vec{\nabla} n|^2$: Originating from the clonal growth mechanism, affects mainly the front dynamics, contributing to their velocity of propagation.

Previous works have identified a valid set of parameter values [25]. These were mainly derived from biological measurements and in part by performing trial and error adjustments to maximise agreement with empirical observations. These are then re-scaled for them to be adimensional and of a similar order of magnitude, thus providing better numerical accuracy:

$$a = 1.39 \quad , \quad b = 1 \quad , \quad \varepsilon = 1.15 \cdot 10^{-2} \quad , \quad \alpha = -1.78 \quad , \quad \delta = 1.03 \cdot 10^{-2} \quad , \quad \beta = -1$$

In these adimensional units, time is adimensionalised with the branching rate: $t' = \omega_b t$, so the mortality is normalised with the branching rate: $\omega = \frac{\omega_{d0} - \omega b}{\omega_b}$.
The simulations will be carried out by integrating Eq. (1) using a pseudo-spectral method.

2.1 Homogeneous steady state

Setting all spatial and temporal derivatives to 0, we will first study the homogeneous steady state solutions:

$$-\omega n + an^2 - bn^3 = 0 \tag{2}$$

Solving this equation we obtain the homogeneous fixed points of the model:

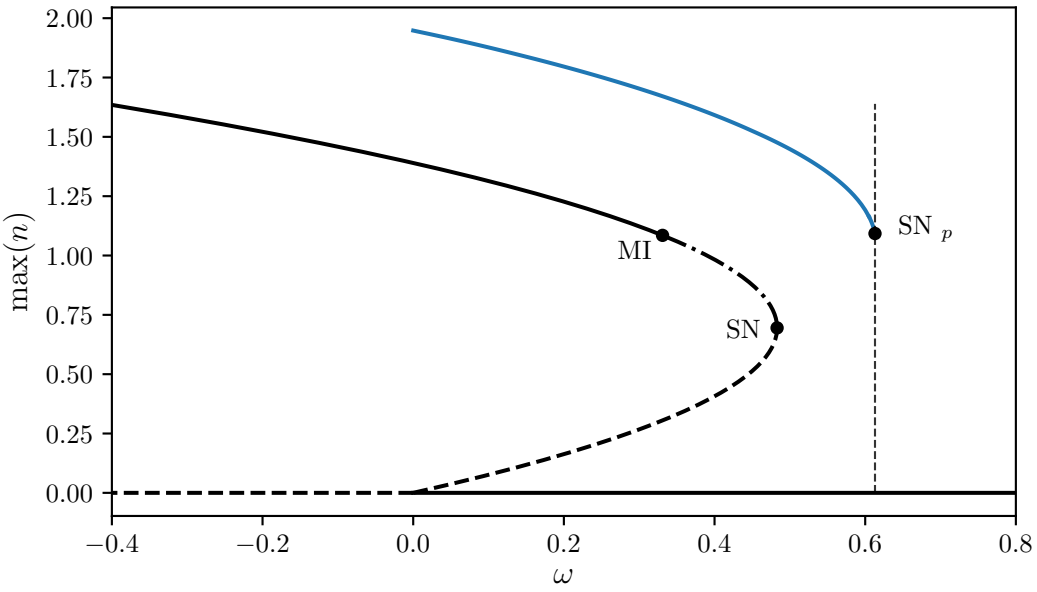

Figure 3: Bifurcation diagram of the clonal growth model in 1D. The continuous black lines correspond to the stable homogeneous fixed points and the dashed lines to the unstable homogeneous fixed points. The Modulation Instability (MI) and Saddle Node (SN) are indicated. The curve that lies between these two points marked with a dotted-dashed line is the part of the homogeneous stable fixed point n_+ that is unstable to patterns, that is, whilst it's stable for homogeneous systems, any heterogeneous perturbation will cause the system to organise into a pattern state. The stable branch for the striped pattern solution, which has been obtained numerically, is shown in blue. Note that here the maximum density is shown, which for the homogeneous solutions corresponds to the total average density, but not for the pattern solutions.

$$\begin{aligned} n_0 &= 0 \\ n_\pm &= \frac{a \pm \sqrt{a^2 - 4b\omega}}{2b} \end{aligned} \tag{3}$$

The first solution, n_0, corresponds to bare soil and is stable for positive mortalities and unstable for negative ones. The other two solutions, $n_\pm$, exist when $\omega < \frac{a^2}{4b}$ (when the radicand is positive) and arise from a saddle-node (SN) bifurcation, being the n_+ solution the node, or stable solution.
The bifurcation diagram corresponding to these solutions is shown in Figure 3. The effect of both non-linear terms can be seen clearly: Due to the $-bn^3$ term, growth is saturated and the equilibrium density is finite, and due to the $+an^2$ term a stable populated solution exists for positive mortalities, although coexisting with the stable bare-soil solution. The biological interpretation of this bi-stability is that once a meadow is established, even if mortality turns positive, facilitative interactions prevent the death of the meadow, whilst an isolated shoot in a region with positive mortality would die. Within this bi-stable region, the unstable branch n_- separates densities for which a meadow would survive and approach the stable populated solution or die and approach the unpopulated solution. This means there is a density threshold (that grows with mortality) for facilitation to overcome the tendency towards extinction due to having a positive mortality. The SN point at $\omega_{SN} = \frac{a^2}{4b}$ acts as a tipping point: If the mortality of a populated meadow increases

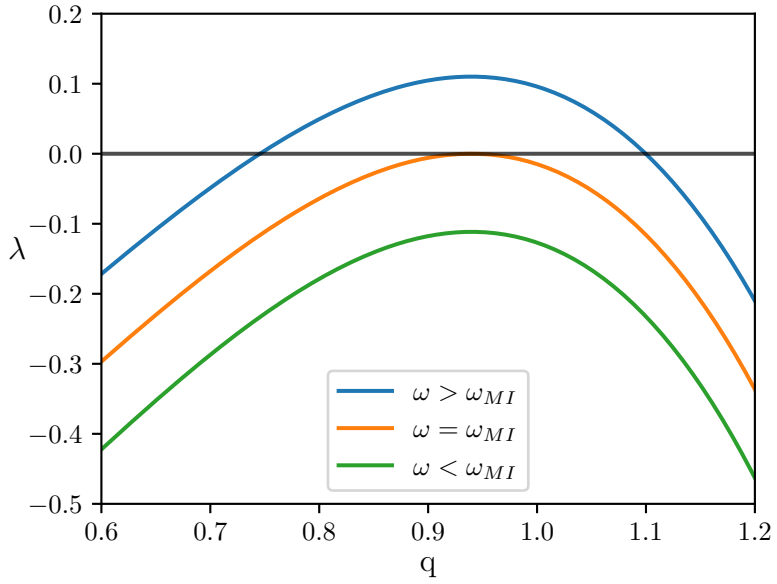

Figure 4: Growth rate λ as a function of the wavenumber q. Three cases of ω are shown: Below, at and above ω_{MI}, as indicated in the legend.

just above this point, bare soil becomes the only stable solution, so the density would fall to zero irreversibly. Even if the mortality were to be decreased back to the previous value, the density would still follow the unpopulated solution branch.

2.2 Patterns

We now recover the spatial terms to study inhomogeneous solutions. Introducing an inhomogeneous perturbation of the form $n_p = Ae^{\lambda t}e^{iqx}$ into Eq. (1) around the fixed point n_+ the expression for the growth rate can be found [29]:

$$\lambda(q) = -\omega + 2an_+ - 3bn_+^2 - \alpha n_+ q^2 + \beta n_+ q^4 - \varepsilon q^2 \tag{4}$$

Where q is the wavenumber of the perturbation. For small values of ω, λ is negative $\forall q$, but, increasing ω, the maximum of $\lambda(q)$ becomes 0, and increasing further there is a range of q for which there is a positive growth rate (Figure 4). This change in sign for the maximum growth rate corresponds to a Turing or Modulation Instability (MI), making the fixed point n_+ unstable to patterns from the first value of mortality where the maximum of $\lambda(q)$ becomes 0 ($\omega_{MI} = 0.331$) up to the SN bifurcation ($\omega_{SN} = 0.483$), where the fixed point disappears. For mortalities in this range, the system self-organises into a stable pattern, which for this model can be stripes or hexagons (positive or negative), depending on the mortality, as can be seen in Figure 5. Although only these three patterns are stable solutions, in reality, mixed patterns are often obtained for random initial conditions of the density field (Figure 5 d). These will eventually converge to one of the three mentioned patterns. Once a pattern is close to being formed, its evolution slows down and defects or fronts between different patterns or orientations of the same type of pattern can persist for a long time.

For simplicity, from now on the simulations will be carried out in a system discretised in a 2×256 grid. Due to the periodic boundary conditions, both grid points along the short direction are identical, giving rise to an effectively 1D system. This makes

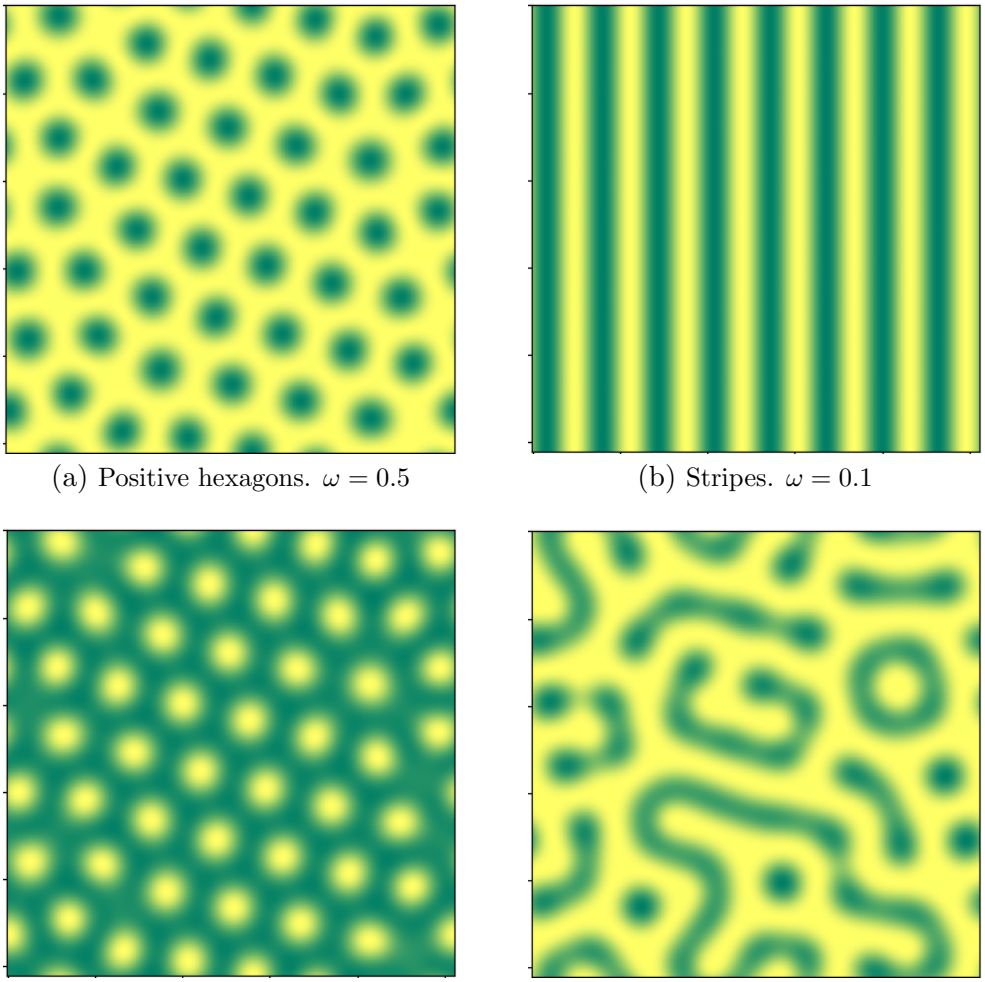

(a) Positive hexagons. $\omega = 0.5$

(b) Stripes. $\omega = 0.1$

(c) Negative hexagons. $\omega = 0$

(d) Mixed. $\omega = 0.35$

Figure 5: Examples of meadows in different patterned states. The three stable configurations are shown (a-c) along with one mixed configuration(d). The mortalities are chosen taking into account the different stability range of each solution. All the simulations were carried out in a 256×256 grid

us lose the hexagonal solutions, and retain only the striped pattern solution. This striped solution corresponds to the blue branch of the bifurcation diagram (Figure 3). Note that the bifurcation diagram shows the maximum density, not the spatial average (which for the homogeneous solution are equivalent). Pattern solutions have generally a larger local density than the equivalent homogeneous meadows for that mortality (when it exists), but a lower average due to the unpopulated regions. The patterned solution exists for values of mortality beyond the SN, up to the patter tipping point $\omega_p \approx 0.612$; self-organisation into patterns increases meadow resiliency. This agrees with the biological reasoning behind pattern formation, which is to better distribute resources when there is some sort of scarcity or pressure. Note that if the mortality is decreased below ω_{MI}, the meadow won't fall back to the homogeneous state until the mortality is decreased even further, down to $\omega = 0$.

3 Theoretical Scenarios

Before attempting to make predictions based on real data, two theoretical scenarios will be tested: a linear increase of mortality and an abrupt change of mortality. The first corresponds to the simplest case of a smooth evolution of mortality, as one would expect from the gradual increase of average temperature due to global warming or other generally continuous changes that might affect the plant such as water pH [23] or salinity [30]. On the other hand, mortality has been found to increase drastically above a certain temperature threshold around $28°C$ [15] and can also increase due to large impact events such as physical aggressions or large runoffs, like the dramatic event in the Dutch Wadden Sea in 1930 [10], where meadows of Zostera Marina, another clonal seagrass, quickly went extinct in that region after the construction of a dam and the incidence of a disease. The study of discontinuous changes in mortality is thus of interest and relevant to realistic scenarios. These two scenarios will offer a qualitative picture of some possible dynamics a meadow can undergo when mortality changes with time.

3.1 Linear increase of mortality

For the first scenario, the mortality will be modelled to depend on time linearly with a certain constant rate of mortality increase $\omega_r \equiv \frac{dw}{dt}$.

$$\omega(t) = \omega_0 + \omega_r t \tag{5}$$

To have a benchmark against which to compare the effect of pattern formation and to see separately the effects of the local non-linearities an^2 and bn^3 from the effects of the spatial terms, we first work with the homogeneous solutions, that is, disregarding all terms with spatial derivatives.

The simulation will be started with a low mortality and the corresponding density from the stable populated branch n_+ as initial condition. We then integrate the model, updating the mortality at each integration step. In Figure 6(a) we can see several runs for different rates of mortality increase, showing the evolution of density with ω. For slow rates, the evolution happens practically along the stable branch of the bifurcation diagram (we can consider the mortality change adiabatic). For faster speeds though, there is not enough time for the solution to approach the steady state before ω changes, so the evolution curve lies above the fixed point curve. In Figure 6(b), the evolution with time is shown. Relative to the simulation length, slower simulations have a more abrupt fall when crossing the SN, whilst for faster ones the crossing of the SN is less appreciable. With equal time-scales, the tail of the faster decays is steeper, as expected, there simply is not a slow section to compare it with. The shape of the tail of the evolution can be approximated by discarding the non-linear terms, since the density is close to 0, the only stable solution beyond the SN.

$$\begin{aligned} \partial_t n &= -\omega_r t n \\ n &= n_0 e^{-\omega_r t^2/2} \end{aligned} \tag{6}$$

The same procedure is now carried out but integrating the whole model including the spatial terms (Eq. (1)). The initial condition will be a homogeneous meadow with a mortality such that the populated homogeneous solution is stable and with

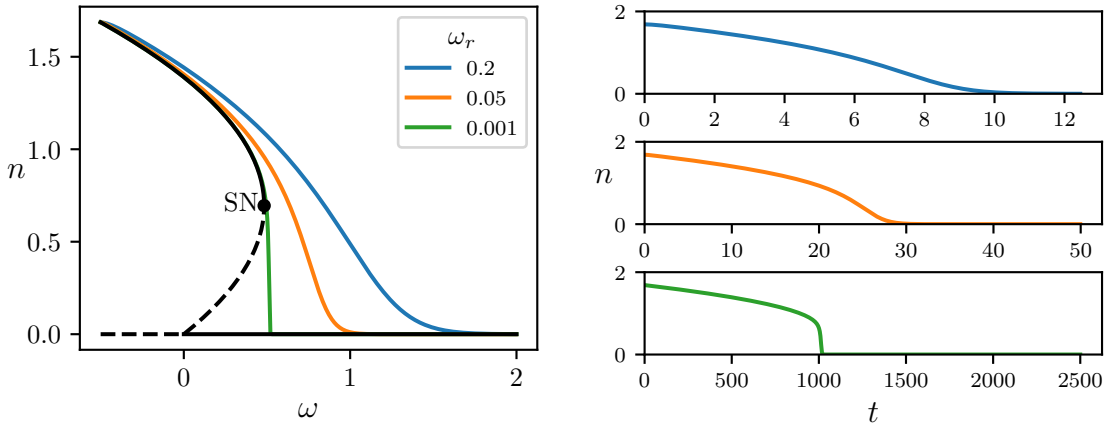

(a) (b)

Figure 6: Density evolution for three simulations using only the homogeneous part of the model with different mortality increase rates, as indicated by legend. The mortality range is $\omega \in [-0.5, 2]$ for all cases. Panel (a) shows the density against the mortality at that point in time, overlaid on the bifurcation diagram. Panel (b) shows the density against time for each simulation.

density corresponding to this stable fixed point. In Figure 7 (a) we can see the evolution of the maximum density with the mortality for different rates ω_r, overlaid on the bifurcation diagram. Here it is clear how the existence of the pattern solution extends the life of the meadow slightly beyond the SN point, which is a tipping point for the homogeneous solution. In Figure 7(b) we can see the results from the same simulation, but this time the average density (not its maximum) against time. Here we can see, especially in the slowest case, how there is a considerable dip in density when changing from one regime to the other, but not complete extinction. The meadow then survives further until reaching the tipping point of the striped solution ω_p.

3.1.1 Threshold in the mortality increase rate for pattern formation

For a fast enough increase in mortality, the meadow does not have time to organise into the striped solution before decaying to the bare-soil solution and "skips" the MI. This can be seen in Figure 7 (a) where, as the rate is increased, the mortality for which the systems transitions to the patterned state is delayed, until skipping it completely for the fastest speed (red curve). Meadows with a mortality increase rate in the region where it might skip the transition to a patterned solution are thus susceptible to small variations in the rate, so finding and understanding this speed threshold is of interest. It can also allow us to either predict if a meadow will develop patterns or not if mortality keeps increasing at a given rate. To find this threshold, we will compare the same simulation with and without the spatial terms. For velocities fast enough to skip the MI, one would expect similar results regardless of the inclusion of the space-dependent terms, since pattern formation does not get a chance to play a significant role. On the other hand, if the speed is slow enough, there should be a noticeable difference since in the full model patterns develop and the tipping point is extended beyond that of the homogeneous model.

To get a value for the lifespan of a meadow, a density under which we consider the

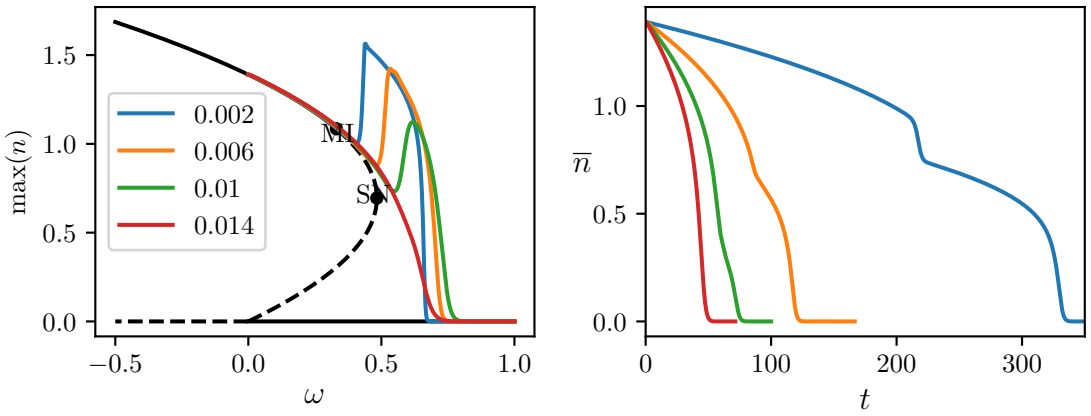

(a) (b)

Figure 7: Evolution of density with a linearly increasing mortality, with four different rates, as indicated in the legend. Panel (a) shows the change in maximum density against mortality. This graph can be misleading since time is implicit, so the time taken to reach the final mortality of $w(t_f) = 1$ for each run is shown in the legend alongside the speed ω_r. The mortality of the striped solution's SN is indicated as a vertical dashed line. Panel (b) shows the change in average density against time for the same four simulations.

meadow to go extinct is chosen ($n_D = 0.01$) and the time for the maximum of the density to dip below it is obtained for different velocities. This time is calculated for both homogeneous and full models, and the discrepancy between the times is calculated as t_{full}/t_{hom}. This discrepancy against the corresponding mortality increase rate is shown in Figure 8, where one can see a very noticeable increase around $\omega_r^T \approx 0.01$. For speeds just slow enough for patterns to form, meadows extend their lifespan by around 20% compared to when patterns do not form for slightly larger speeds. This value depends on the somewhat arbitrary choice of the density n_D below which the meadow is considered to die, but the existence and position of the threshold in the mortality rate for pattern formation does not depend on n_D as long as it is reasonably smaller than the density of a stable populated meadow.

This threshold can be understood by comparing the time the system takes to jump to the pattern solution (determined by the unstable eigenvalue of the MI) with the time the mortality takes to reach the SN. If the latter is shorter the system jumps to the bare solution, otherwise, the patterns develop and the tipping point is avoided. We will now estimate both characteristic times to be able to compare them. In general, for a starting value near an unstable fixed point, the growth of this perturbation can be approximated by an exponential increase with the eigenvalue of the fixed point. In our case, the eigenvalue changes with time, since it depends on ω, which is time-dependent. We will not use the exact eigenvalue, since it has a dependence on the wavenumber q, instead, we will use an approximate growth rate $\sigma(t)$ assuming the maximum of the dispersion relation ($\lambda(q)$ in Eq. (4)) dominates the growth rate: $\sigma(t) = \max_q[\lambda(q, \omega(t)]$. The evolution of a perturbation to n_+ will be the solution to the following equation:

$$\partial_t n_p = \sigma(t) n_p \tag{7}$$

From the expression of $\lambda(q)$ (Eq. (4)), we can calculate σ analytically:

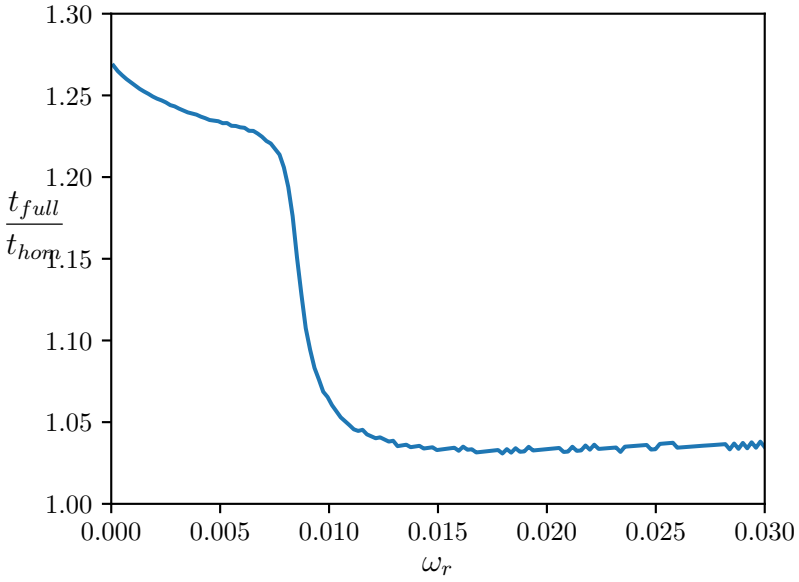

Figure 8: Ratio of lifespan with and without spatial terms for simulated meadows against the corresponding mortality increase rate.

$$\sigma = -\omega + 2an_+ - 3bn_+^2 - \frac{1}{4}\frac{(\alpha n_+ + \varepsilon)^2}{\beta n_+} \tag{8}$$

In Figure 9a we plot $\sigma(\omega)$, where we can see that the dependence is close to linear except for the last small section towards ω_{SN}. Approximating the dependence linearly, we obtain a reasonable approximation: $\sigma(\omega) \approx 3.23\omega + \text{ct}$. By choosing to start at the MI ($\omega(0) = \omega_{MI}$) we have that $\sigma(0) = 0$, since, by definition, the maximum growth rate is 0 at the MI. This allows us to ignore the constant term. Since $\omega(t) = \omega_r t + \omega_0$, we obtain the final expression for $\sigma(t)$:

$$\sigma(t) \approx 3.23\omega_r t \equiv \sigma_s t \tag{9}$$

Introducing (9) into (7) and solving:

$$\begin{aligned} \partial_t n_p &= \sigma_s t n \\ n_p(t) &= n_0 e^{\frac{\sigma_s t^2}{2}} \end{aligned} \tag{10}$$

A constant eigenvalue λ has an associated characteristic time of $\tau = \frac{1}{\lambda}$, which is the time taken for the distance to a fixed point to increase or decrease by a factor of $e = 2.718$. From the same definition, we define, for our time-dependent case, the fixed point's escape time τ_e. The assumption is that after a time of this order, the system escapes the influence of the fixed point, in this case forming patterns if this happens before the SN is crossed:

$$\begin{aligned} n_p(\tau_e) = n_0 e^{\frac{\sigma_s \tau_e^2}{2}} &= e n_0 \\ 1 &= \sigma_s \tau_e^2 / 2 \\ \tau_e &= \sqrt{\frac{2}{\sigma_s}} \end{aligned} \tag{11}$$

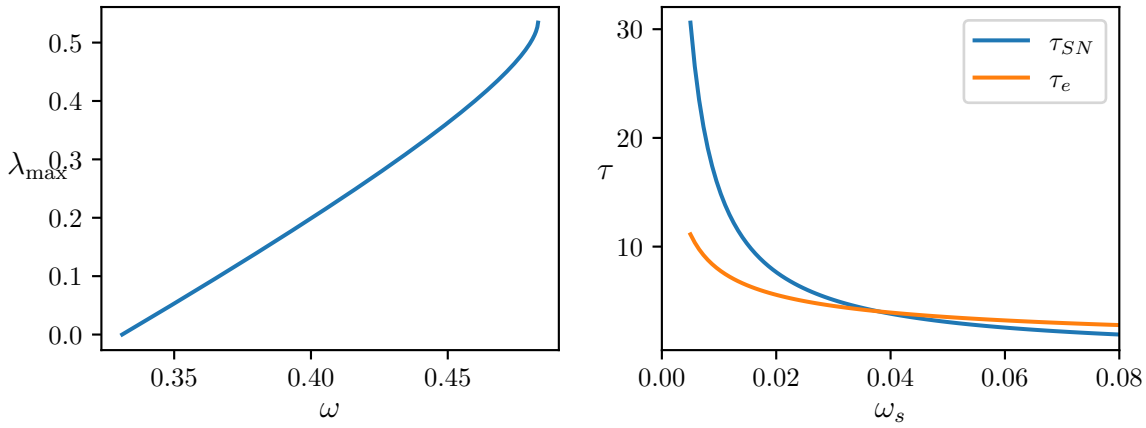

(a) (b)

Figure 9: (a) Maximum growth rate against mortality in the range where n_+ is unstable to patterns. (b) Characteristic time for both ways to exit the fixed point n_+ with a linearly increasing mortality, as a function of the mortality speed.

The second timescale, is simply the time taken to get from the MI to the SN with a constant mortality speed ω_r:

$$\tau_{SN} = \frac{\omega_{SN} - \omega_{MI}}{\omega_r} \tag{12}$$

In Figure 9b we plot the values of τ_e and τ_{SN} for a range of values of ω_r, on which both depend. We can see how, for slow mortality speeds, the time to escape the fixed point τ_e is much smaller than the time to reach the SN τ_{SN}, so the meadow organises into a pattern solution way before crossing the SN. Around the same order of magnitude of the threshold value of $\omega_r^T \approx 0.01$ found in the simulation, both times approach each other, finally crossing each other around $\omega_r^T = 0.038$. There is some arbitrariness in the estimation of the characteristic time τ_e, which only gives a value of the order of magnitude, hence the discrepancy in the theoretical and numerical values found, which are nonetheless of the same order of magnitude.

Pattern formation is generally understood as an indicator of ecosystem health and a mechanism of resilience [31]. For a rapidly increasing mortality, not only is this resilience lost, but no visible warning of the meadow's situation is given.

3.2 Abrupt change of mortality

We will now study an abrupt increase in mortality. For this, the initial condition will be a density field corresponding to a stable populated meadow, but the mortality will be set to a constant value beyond the tipping point. As before, we will first work with the homogeneous model and then with the full one.

For the homogeneous model, a large density is set as initial condition and the mortality is fixed beyond the SN. As mentioned in the introduction, the calculation of ω from field data and predictions of the density evolution have been performed using a linear model equivalent to linearising around the fixed point n_0 corresponding to the bare soil solution. Our results will be compared to what would be obtained with this linear model, which yields an exponential decay with ω:

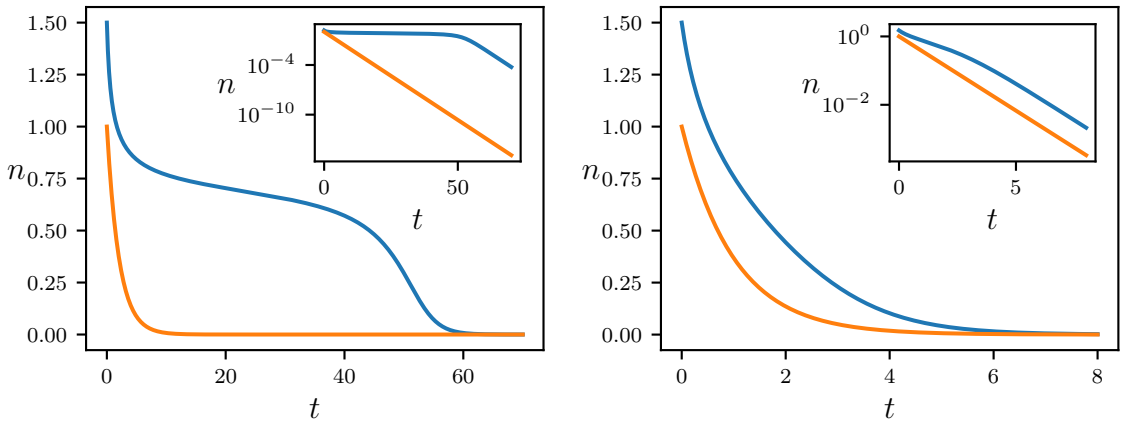

(a) $\omega = 0.49$ (b) $\omega = 1$

Figure 10: Time evolution of the density with a constant mortality such that the only solution is bare soil, starting from a populated meadow. In orange the decay predicted by the linear model is shown, and in blue the one predicted by the homogeneous non-linear model. Panel (a) corresponds to a mortality just above the SN and Panel (b) a mortality considerably larger.

$$n(t) = n_0 e^{-\omega t} \tag{13}$$

This will allow us to compare with what could be predicted using linear models and see separately the effects of the non-linear terms. In Figure 10 we can see the time evolution of the density for both the linearised and non-linear (homogeneous) models, for values of ω just above the SN (Figure 10a) and a larger value of ω (Figure 10b). The inset shows the same plots with logarithmic y-axes. There, one can see how, for small values of the density, the non-linear model indeed follows an exponential decay as in the linear approximation. However, at the beginning of the evolution, where densities are larger and non-linear terms dominate, there is a considerable deviation from the exponential behaviour.

Whilst the non-linearities cause meadows to take longer to die off, even for mortalities where there are no stable populated solutions, they can also cause empirical estimations of the mortality for meadows just beyond the critical point to be underestimated if using the linear model to extract the mortality from measurements of $\partial_t n$: One would predict a low mortality for a meadow which is actually on its road to extinction if the meadow is in the slowed-down region, since the measured slope would be lower than expected.

The simulations are now repeated including the spatial terms. The scenario will be that of a meadow in a stable pattern state whose mortality is increased suddenly beyond ω_p. To generate the initial condition, a simulation is carried out with a mortality for which the pattern solution is stable, letting enough time for the simulated meadow to reach the steady state which will serve as initial condition. The mortality is then chosen such that the striped solution no longer exists. In Figure 11, the time evolution of the meadow's average density with a mortality just above the tipping for the patterned solution is plotted, along with a raster plot showing the 1D density profile at each point in time. There are several density dips, followed

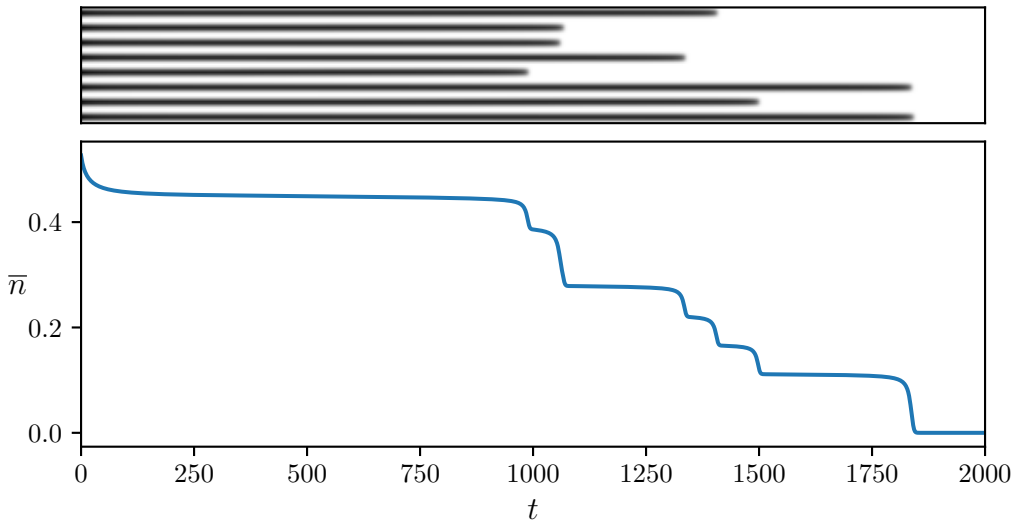

Figure 11: Time evolution of density of 1D system starting with the stable pattern solution for $\omega = 0.6$, but with $\omega = 0.6135$, just beyond the tipping point. The bottom panel shows the evolution of the average density, whilst the top panel is a raster plot showing the 1D density field at each point in time. Each black line corresponds to a peak in the field, with each existing for a different amount of time. The dips in the average density coincide with the disappearance of peaks as seen in the raster plot.

by a plateau that corresponds to meta-stable configurations that survive for some time. Each dip in density corresponds to the loss of a peak or pair of peaks, as can be seen in the corresponding raster plot. These meta-stable configurations are only found when the mortality is very near the SN. When the mortality is larger, the whole meadow disappears more uniformly, as can be seen in Figure 12a, where the evolution of the average density does not show the same plateaus and dips as in the previous case. Nonetheless, the decay is not completely uniform as some peaks decay at slightly different rates, as evidenced in Figure 12b, where the density profile at an intermediate step of the decay is shown and all peaks have different heights. This spatial variability for the density even when the mortality is the same for the whole meadow loss highlights the importance of taking measurements at different points in a meadow in order to obtain a clear picture of its dynamics, along with observing the large scale spatial structure of the meadow.

3.3 Homogeneous model as a dynamical system

When working with the homogeneous 1D version of the model and with a linearly time-dependent mortality, the differential equation can be transformed into a 2D dynamical system:

$$\begin{aligned} \dot{n} &= -\omega n + an^2 - bn^3 \\ \dot{\omega} &= \omega_r \end{aligned} \tag{14}$$

This representation can help us discuss some of the phenomena both for the abrupt change and linearly increasing mortality cases more formally and visualise the whole phase space for a given velocity, instead of a single trajectory. The phase space for this dynamical system has the same coordinates as the bifurcation diagram of the homogeneous solutions shown in Figure 3, so the dynamics on this phase space are

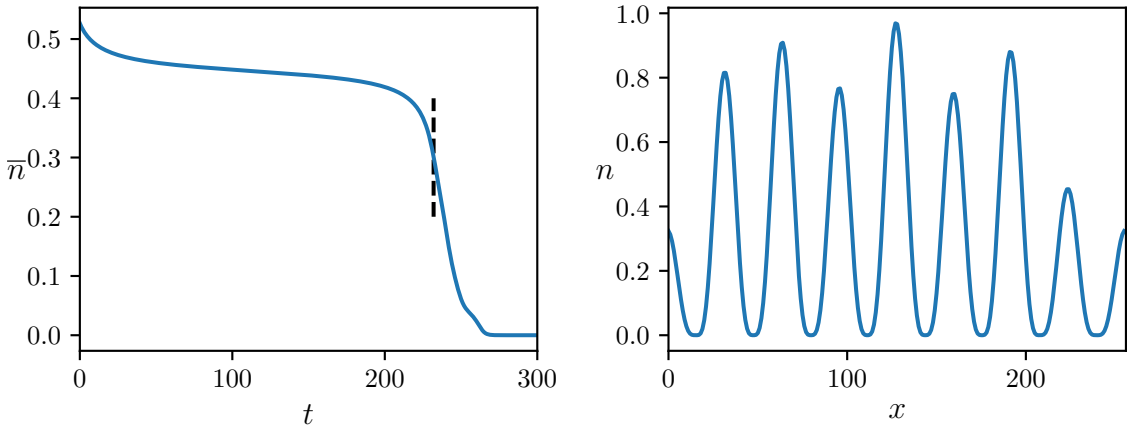

(a) (b)

Figure 12: (a) Time evolution of the density with $\omega = 0.614$ (b)Density profile of a meadow after some evolution ($t = 63$), before reaching extinction, showing that decrease is not uniform across all peaks, which started with the same height at $t = 0$.

identical to those shown in Sections 3.1 and 3.2 with the homogeneous system when representing n against ω.

The condition for fixed points is that both $\dot{n} = 0$ and $\dot{\omega} = 0$. The solution of the first condition is the solution to the homogeneous stationary equation given in Eq. (3), whilst the second condition implies that $\omega_r = 0$, that is, fixed points only exist for a constant mortality and these coincide with the stationary solutions in the bifurcation diagram. When mortality is time dependent, the stationary solutions in the bifurcation diagram are the nullclines of n and there are no fixed points.

For the $\omega_r = 0$ case, shown in Figure 13(a), one can see clearly how n_- separates densities for which facilitation is enough to take the system to the populated state n_+ from those where it is not enough and the system falls to the bare soil solution. Trajectories with $\omega \gtrsim \omega_{SN}$ fall to the bare soil solution, but do so passing near the fixed point n_+, hence the reason why the critical slowing down is observed in the simulations for an abrupt change of mortality with mortality slightly above the SN.

The $\omega_r > 0$ case, shown in Figure 13(b), shows no fixed points, with all initial conditions approaching $n = 0$ and $\omega \to \infty$. Since the stationary solutions on the bifurcation diagram are the nullclines of n, the behaviour in the vertical direction is still guided by these fixed points and will slow down near them. As ω_r is increased, its contribution to the velocity in phase space grows and the effects of the non-linear terms, such as critical slowing down or the sharp fall when the SN is crossed, are obfuscated. Unlike what one would have with actual fixed points, a trajectory can cross any of the fixed point lines under certain conditions, for example, if the initial density is below n_+ and ω_r is fast enough.

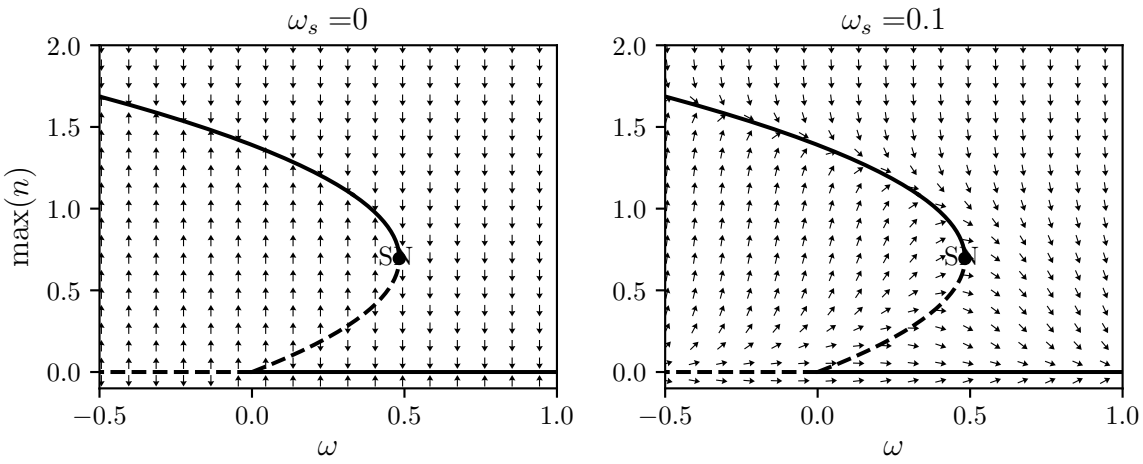

Figure 13: Phase space of the homogeneous model with a constant mortality speed in dynamical system form given in Eq. (13) for the $\omega_r = 0$ (a) and $\omega_r > 0$ (b) cases.

4 Real data

Now that the basic scenarios have been explored, we can implement real predictions of the evolution of mortality to estimate the future change in the studied meadows. As mentioned in the introduction, predictions for the decline in *P. Oceanica* meadows due to the increase in mortality caused by global warming have been made [16] based on field data presented in a previous article [13]. We will use the same mortality time series, corrected and in the appropriate units for our model.

4.1 Data acquisition

From 2002 to 2006 the water temperature in several *P. Oceanica* meadows along the coast of the isle of Cabrera, in the homonymous archipelago located to the south of Mallorca, were measured regularly, along with roughly yearly measurements of the density change in delimited parcels of the meadows [13]. The Cabreran archipelago is a natural park, so direct anthropogenic pressures are expected to be lower than in other coastal areas, making it a good place to study the effect of temperature rise. Living shoots were marked with a plastic tag, so each measurement allowed for the counting of surviving (alive with a tag), dead (dead with a tag) and new shoots (alive without a tag). The shoot mortality is estimated for each measurement, comparing the number of surviving shoots at a given measurement $N_S(t_i)$ with the total from the previous measurement $N_T(t_{i-1})$

$$M = \frac{1}{\Delta t} \ln \left[\frac{N_T(t_{i-1})}{N_S(t_i)} \right] \tag{15}$$

Note that, by construction, M cannot be negative since the surviving shoots $N_S(t_i)$ will always be less than or equal to the previous total shoots $N_T(t_{i-1})$.
The Recruitment rate (analogous to the branching coefficient ω_b in our model) is calculated by comparing the current total shoot count $N_T(t_i)$ to the number of surviving shoots $N_S(t_i)$, measuring the proportion of alive shoots that are new:

$$R = \frac{1}{\Delta t} \ln \left[\frac{N_T(t_i)}{N_S(t_i)} \right] \tag{16}$$

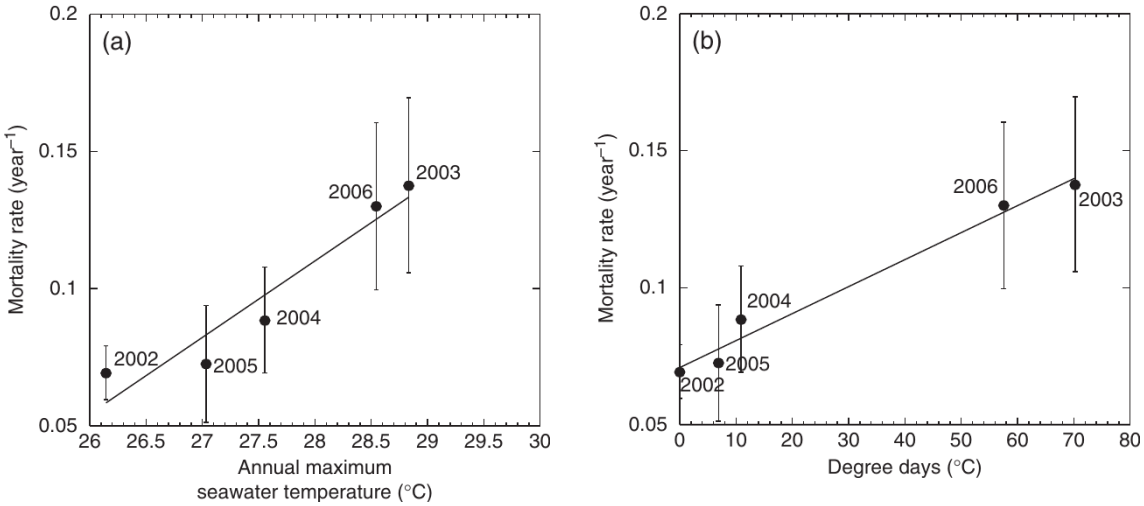

Figure 14: Recorded mortality for each year against the respective maximum temperature (a) or temperature anomaly over 26.6°C in degree days (b) [13]

.

The net shoot mortality W is defined as the difference between the mortality and recruitment rates:

$$\begin{aligned} W = M - R &= \frac{1}{\Delta t} \ln \left[\frac{N_T(t_i - 1)}{N_S(t_i)} \frac{N_S(t_i)}{N_T(t_i)} \right] \\ &= \frac{1}{\Delta t} \ln \left[\frac{N_T(t_{i-1})}{N_T(t_i)} \right] \end{aligned} \tag{17}$$

What effectively is being measured is the change in density, which is fitted to an exponential decay, as predicted by a linear population model.
In total, 9 parcels at different locations amongst 3 meadows were studied. The average mortalities obtained with this method were then plotted against the corresponding annual maximum seawater surface temperature ($\mathrm{SST_{max}}$) and the temperature anomaly with respect to the 1988-1999 average maximum of 26.6°C in degree-days, as shown in Figure 14. In both cases, a positive correlation was observed and a linear was fit made. In the follow-up article [13], only the results of the fit with respect to $\mathrm{SST_{max}}$ are used. For this reason and due to the availability of predictions of $\mathrm{SST_{max}}$, we will also only use that fit. Their fit obtained for the shoot mortality in y^{-1} with $\mathrm{SST_{max}}$ gave the following linear relationship:

$$\begin{aligned} M &= a \cdot \mathrm{SST_{max}} + b \\ a &= \quad 0.021 \pm 0.002 \\ b &= -0.47 \pm 0.06 \end{aligned} \tag{18}$$

Using historical data of $\mathrm{SST_{max}}$, predictions of the evolution of atmospheric greenhouse gas concentration and atmospheric-ocean models, predictions of the increase of $\mathrm{SST_{max}}$ until the end of the 21st century were made, as shown in Figure 15. Introducing this $\mathrm{SST_{max}}$ time series into Eq. (18), a time series for mortality M can be obtained. Finally, the recruitment rate must be subtracted from the mortality M to obtain the net shoot mortality $W = M - R$. The recruitment rate was considered independent of temperature and estimated as $R = 0.05 \pm 0.01 y^{-1}$.

For simplicity, the temperature time series has been modelled by fitting linearly the ensemble average of predicted $\mathrm{SST}_{\max}$ growth (red line in Figure 15) and adding a Gaussian noise with standard deviation such that the fluctuations are of the same size as in the prediction:

$$\begin{aligned} \mathrm{SST}_{\max} &= 0.04\mathrm{Y} - 53.2 + \eta \\ \sigma(\eta) &= 0.24 \end{aligned} \tag{19}$$

With this we can finally generate a time series of mortality which we will use to perform simulations.

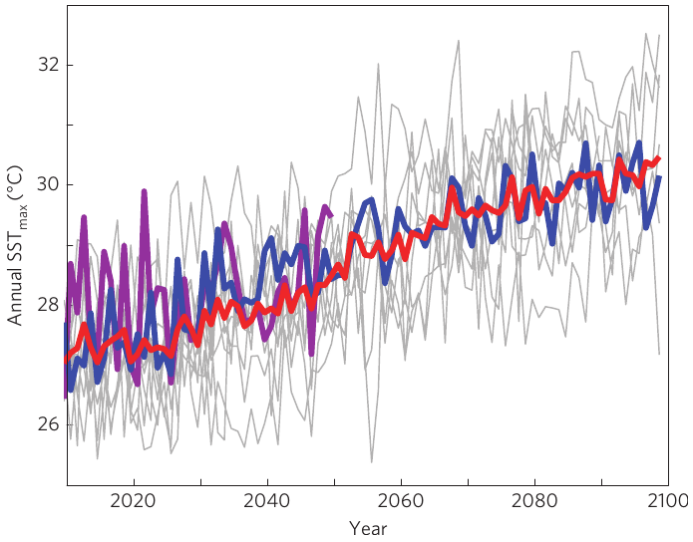

Figure 15: Annual $\mathrm{SST}_{\max}$ in the Balearic Islands region projected for the twenty-first century. Grey lines: the outputs of single general Atmospheric-Ocean General Circulation Models (AOGCMs) models; purple and blue lines, respectively: the outputs of PROTHEUS and VANIMEDAT2 (regional) models; red line: the ensemble average [16]

4.2 Correction to measured mortality

Before introducing the mortality time series into the clonal growth model, a few adjustments must be made. Due to the choice of the adimensionalisation of the model's parameters, the mortality needs to be adimensionalised by dividing by the recruitment rate $W' = \frac{W}{R}$. Time is also re-scaled multiplying by the recruitment rate ($t' = Rt$). This means that one unit of time in the simulation corresponds to $\frac{1}{R} = 20$ years.

Measurements of mortality have been made assuming a linear model:

$$\partial_t n = -\omega_L n \tag{20}$$

We cannot simply take the values of mortality obtained there, since the non-linear terms have not been taken into account when translating the density measurements into mortality values. We will now obtain a relationship between the values calculated assuming the linear model (ω_L) and the mortality that will be used in the model (ω_{NL}). There is no mention of the meadows' spatial arrangement so, for simplicity, we will assume it is in the homogeneous regime, which seems likely looking at

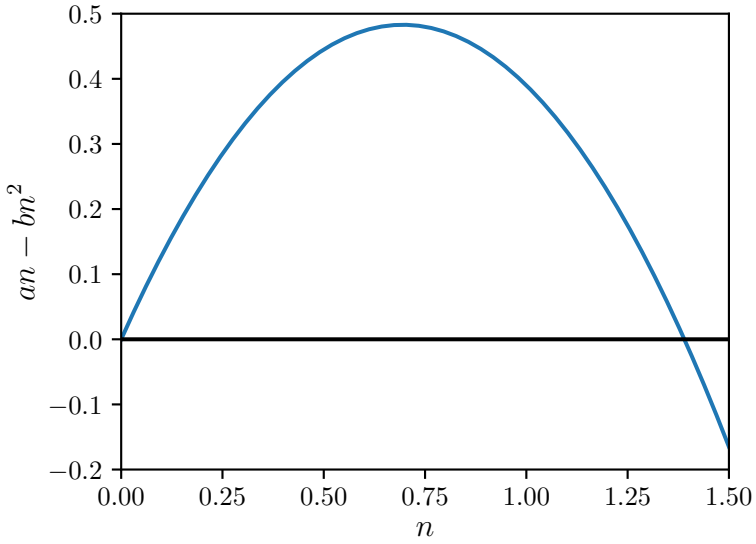

Figure 16: Size of the correction to the linearly measured mortality as a function of the meadow density.

the meadow cartography [8]. We factor out n from the linear homogeneous equation to express it as follows:

$$\partial_t n = \left(-\omega_{NL} + an - bn^2\right) n \tag{21}$$

By comparing Eqs. (20) and (21), taking into account $\partial_t n$ and n are experimental measures and as such will be the same in both models, we can see that the terms multiplying n on both equations must be equal:

$$-\omega_L = -\omega_{NL} + an - bn^2 \tag{22}$$

Finally, we rearrange Eq. (22) to obtain an expression for ω_{NL} in terms of ω_L:

$$\omega_{NL} = \omega_L + an - bn^2 \tag{23}$$

The correction $(an - bn^2)$ which is added to the linearly measured mortality has a maximum value which coincides with $\omega_{SN} = 0.482$, and becomes 0 at $n = a = 1.39$, as can be seen in Figure 16. After this density, which is the same a stable homogeneous meadow would have at mortality $\omega = 0$, the correction becomes negative. For any measured positive mortality, the actual mortality will be larger (assuming the meadow's density is near or below its equilibrium value). Not considering the non-linearities causes the mortality to be underestimated: facilitation causes a slower decay that is erroneously attributed to a lower mortality.

The mortality data which we are using [13] is an average for several sites and depths with initial densities ranging from 140 to 820 shoots m^{-2}, with an average value of $n(2002) = 430 \pm 210 \text{shoots} m^{-2}$. This large difference is mainly due to the different depths, which ranged from 5m to 25m, with deeper meadows having consistently lower densities, since less light can arrive. To adimensionalise this value we have to divide by $\sqrt{\frac{\omega_b}{b}}$, with $b = 12.5$ cm^4 y^{-1} and $\omega_b = R = 0.05 \pm 0.01 \text{y}^{-1}$. The range of initial densities in adimensional units goes from 0.2 to 1.3. The simulations will require a starting density, and this in turn affects the initial mortality ω_{NL}.

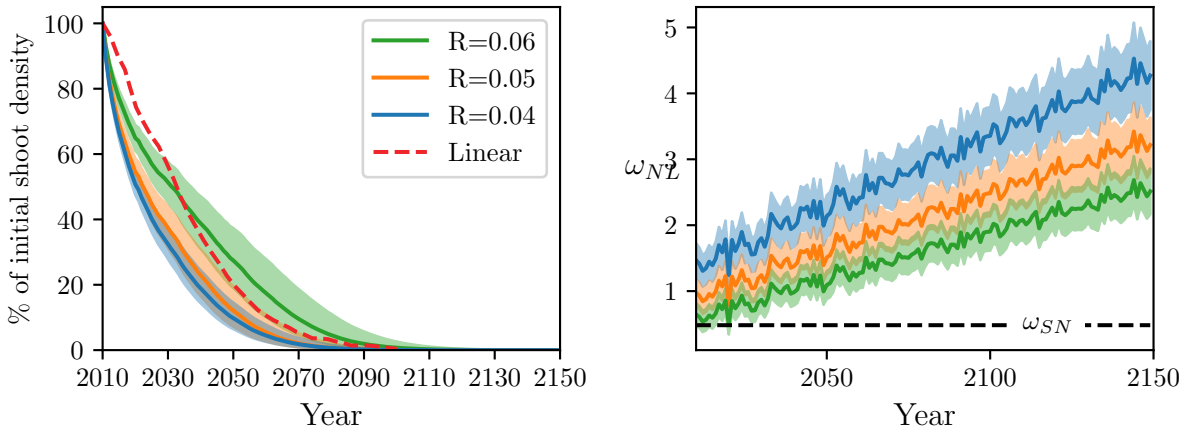

Figure 17: Evolution of the density (a) and mortality (b) of a meadow with an increasing mortality as predicted in [16]. The three colours correspond to three values of the recruitment rate R, accounting for the error given. The region between the upper and lower bounds taking into account the error in the mortality fit (Eq. (18)). The prediction given in [16] is shown as a red dashed line.

4.3 Simulation with real data

At last, we proceed to simulate the evolution of a meadow under the described rise of mortality due to global warming using the clonal growth model. Since $\mathrm{SST}_{\max}$ is calculated for each year, a 1 year run with constant mortality is carried out for each year, with the final state becoming the initial state of the next year with its corresponding mortality. In each step, the mortality will be taken from the predicted mortality time series and corrected taking into account the current average density. The two sources of error considered are the error in the fit of W against $\mathrm{SST}_{\max}$ and the error in the recruitment rate R. Simulations will be made using the central value and the upper and lower bounds according to the errors, giving in total 9 simulations covering all combinations of errors for both sources considered.
In Figure 17a we can see the evolution of a meadow for $R = 0.04, 0.05$ and 0.06, each case showing the uncertainty range due to the error in W. For comparison, the curve predicted with the linear model [16] is also shown. In this case, there is not a large difference between both models. To better comment on this, it is illustrative to see the evolution of mortality with time (Figure 17b). Though the measured mortality is extrapolated linearly, due to the density-dependent correction, the corrected mortality does not follow a linear relationship with time, especially at the beginning of evolution where the density (and hence the correction) is not negligible. Via a linear fit to the curve corresponding to the central value, the approximate mortality rate of increase is found to be $\omega_r = 0.37 \pm 0.05$, much larger than the threshold speed for the MI of $\omega_r^T \approx 0.01$, so it is reasonable to assume that these meadows won't form patterns. Almost every scenario starts with a mortality beyond ω_{SN}, due to this, together with the large mortality increase rate, the evolution is similar to that predicted by the linear model.

5 Conclusions

We have studied the clonal growth model to describe the spatiotemporal dynamics of *P. Oceanica* meadows including non-linear and spatial terms arising from collective interactions. This model presents complex phenomena such as pattern formation, tipping points and hysteresis. The main focus has been on the long term response of meadows when the mortality increases with time.

The regimes of this model have been summarised in the bifurcation diagram, which presents a sub-critical saddle-node bifurcation at positive mortalities, giving rise to a region of bi-stability where meadows can exist despite the positive mortality thanks to the collective facilitation. We have found a Modulation Instability in the stable branch that makes homogeneous meadows unstable to patterns above this mortality. The branch in the bifurcation diagram corresponding to the pattern state has a tipping point at a higher mortality than the homogeneous meadow, implying that pattern formation serves as a resiliency mechanism.
To get an overview of the possible dynamics, simulations have been carried out with both a continuous linear increase and with an abrupt increase of mortality. When the mortality increases linearly with time, the density of the meadow is close to the stable one at that mortality for slow rates of mortality increase, so when representing density against mortality, the curve lies almost on the bifurcation diagram. For faster speeds, the actual density lags behind the stable one, not having enough time to settle onto the stable density before the mortality increases. Once the tipping point is crossed and the only solution is bare soil, the impact of the non-linear terms is reduced and the decay is close to an exponential decay with t^2. When increasing the mortality past the Modulation Instability, the homogeneous meadows start to organise into a spatially heterogeneous state, "jumping" to another branch of the bifurcation diagram whose tipping point is for a larger mortality. The jump to the branch does not happen immediately after crossing the MI, but there is a delay that becomes bigger the larger the mortality increase is. If the speed at which mortality is being increased is too fast, the meadow does not have enough time to develop patterns before crossing the homogeneous tipping point and decaying to the bare solution. We have found numerically and estimated analytically a threshold value above which the system does not benefit from the increased resiliency of pattern formation. This speed threshold has been interpreted as the result of a time scales separation amongst the escape time from the unstable homogeneous solution when it is unstable to patterns and the time taken to reach the homogeneous tipping point due to the increase of mortality. Bifurcations are often studied assuming slow changes of the bifurcation parameter, so more studies in this type of dynamic bifurcations are of interest, especially bearing in mind its likely application to real-world systems, where control parameters are changed non-adiabatically.

When the mortality is increased abruptly, from one yielding a stable meadow to one where bare soil is the only solution, we have found a critical slowing down for mortalities above but near the SN, with densities decreasing slower than expected for values near the density at the SN. This can be understood better when expressing the homogeneous part of the model with a time-dependent mortality as a dynamical system, where the general theory regarding trajectories in phase space near a fixed point justifies the existence and position of this slowing-down. For larger mortalities, the evolution resembles more an exponential decay, especially when densities

become small enough for non-linear effects to be negligible. When the meadow is initially in a patterned state and the mortality is just above the SN for the pattern branch, peaks disappear at different times and meta-stable configurations of few peaks can exist for long times.

Based on previous works collecting and extrapolating field data using a linear approximation, we have attempted to make predictions with the same data but using the clonal growth model. A correction has been obtained to translate the measurements using the linear model into mortalities valid for our model, and we have simulated the evolution of the studied meadows. Several simulations have been carried out with different parameter values accounting for several error sources.
In general, there is not a stark difference between the previous predictions with a linear model and ours. This is mainly due to the large starting mortality, beyond the SN, and large increase rate, annulling most of the improved resiliency from facilitation and crossing the MI so fast that patterns do not form. Another important factor is that the correction to the mortalities measured using a linear model underestimate the intrinsic mortality, so the simulations with the linear model had lower mortality values. The 9 meadows studied offer a very small amount of measurements (4 or 5, which get reduced by one since time differences are taken) so the average from these 9 meadows was used. This might be problematic since the meadows were at different depths and so cannot be considered equivalent, despite being in the same region.

Overall, the quantitative estimations are to be taken with great caution. Despite this lack of firm quantitative values presented, a general sketch of the possible scenarios has been explored and the precautions that must be taken in order to capture and predict the correct situation of meadows have been highlighted, especially those regarding to the use of only local measurements without regarding the larger-scale structure and the exclusion of non-linear terms when extracting mortality values from data. Future work will involve working directly with larger and longer datasets with a more rigorous approach to error prediction and extrapolation. Future work should also consider a 2D space, since all the work here has been made in a 1D system. Other models with less approximations and more free parameters can also allow for a more exact simulation.

Measurements of shoot density change are hard to scale up since they have to be carried out by diving in the region and manually counting shoots in the parcelled-out area. This direct solution to this limitation is evident: more investment in monitoring programs, but it is not the only one. Technological developments can give us better remote sensing techniques to automate these measurements and are already used to study the large-scale structure of meadows, at a resolution that is more than enough to study the patterns formed by these meadows [8]. Citizen science projects are also being developed by NGOs such as Medgardens [32] or Save the Med [33], both based in the Balearic Islands, in order to empower non-scientists to learn the techniques to monitor *P. Oceanica* meadows. This can have the dual effect of increasing the available data dramatically and approaching the general public to the often too gated scientific community and the reality of our seas.
We are all in this together, so it makes sense to involve as many people as possible in the task of understanding and protecting the vital ecosystems on which we and uncountable other beings depend.

References

[1] V. Pasqualini, C. Pergent-Martini, P. Clabaut, and G. Pergent. Mapping ofPosidonia oceanicausing aerial photographs and side scan sonar: Application off the island of corsica (france). *Estuarine, Coastal and Shelf Science*, 47(3):359–367, September 1998.

[2] Carlos M. Duarte, Iñigo J. Losada, Iris E. Hendriks, Inés Mazarrasa, and Núria Marbà. The role of coastal plant communities for climate change mitigation and adaptation. *Nature Climate Change*, 3(11):961–968, October 2013.

[3] Carlos M. Duarte, Hilary Kennedy, Núria Marbà, and Iris Hendriks. Assessing the capacity of seagrass meadows for carbon burial: Current limitations and future strategies. *Ocean & Coastal Management*, 83:32–38, October 2013.

[4] C. M. Duarte, J. J. Middelburg, and N. Caraco. Major role of marine vegetation on the oceanic carbon cycle. *Biogeosciences*, 2(1):1–8, February 2005.

[5] Sophie Arnaud-Haond, Carlos M. Duarte, Elena Diaz-Almela, Núria Marbà, Tomas Sintes, and Ester A. Serrão. Implications of extreme life span in clonal organisms: Millenary clones in meadows of the threatened seagrass posidonia oceanica. *PLoS ONE*, 7(2):e30454, February 2012.

[6] Claudio Lo Iacono, Miguel Angel Mateo, Eulàlia Gràcia, Lluis Guasch, Ramon Carbonell, Laura Serrano, Oscar Serrano, and Juanjo Dañobeitia. Very high-resolution seismo-acoustic imaging of seagrass meadows (mediterranean sea): Implications for carbon sink estimates. *Geophysical Research Letters*, 35(18), September 2008.

[7] Ehud Meron. *Nonlinear Physics of Ecosystems*. CRC Press, April 2015.

[8] CAIB. Projecte life posidonia. `lifeposidonia.caib.es/user/index_ct.htm`.

[9] Núria Marbà, Elena Díaz-Almela, and Carlos M. Duarte. Mediterranean seagrass (posidonia oceanica) loss between 1842 and 2009. *Biological Conservation*, 176:183–190, August 2014.

[10] Tjisse van der Heide, Egbert H. van Nes, Gertjan W. Geerling, Alfons J. P. Smolders, Tjeerd J. Bouma, and Marieke M. van Katwijk. Positive feedbacks in seagrass ecosystems: Implications for success in conservation and restoration. *Ecosystems*, 10(8):1311–1322, October 2007.

[11] Carlos M. Duarte, Tomás Sintes, and Núria Marbà. Assessing the co2 capture potential of seagrass restoration projects. *Journal of Applied Ecology*, 50(6):1341–1349, September 2013.

[12] Núria Marbà, Carlos M. Duarte, Marianne Holmer, Regino Martínez, Gotzon Basterretxea, Alejandro Orfila, Antoni Jordi, and Joaquín Tintoré. Effectiveness of protection of seagrass (posidonia oceanica) populations in cabrera national park (spain). *Environmental Conservation*, 29(4):509–518, December 2002.

[13] Núria Marbà and Carlos M. Duarte. Mediterranean warming triggers seagrass (posidonia oceanica) shoot mortality. *Global Change Biology*, 16(8):2366–2375, November 2009.

[14] Elena Díaz-Almela, Núria Marbà, Regino Martínez, Rocío Santiago, and Carlos M. Duarte. Seasonal dynamics of posidonia oceanica in magalluf bay (mallorca, spain): Temperature effects on seagrass mortality. *Limnology and Oceanography*, 54(6):2170–2182, August 2009.

[15] Ioannis Savva, Scott Bennett, Guillem Roca, Gabriel Jordà, and Núria Marbà. Thermal tolerance of mediterranean marine macrophytes: Vulnerability to global warming. *Ecology and Evolution*, 8(23):12032–12043, November 2018.

[16] Gabriel Jordà, Núria Marbà, and Carlos M. Duarte. Mediterranean seagrass vulnerable to regional climate warming. *Nature Climate Change*, 2(11):821–824, May 2012.

[17] Max Rietkerk and Johan van de Koppel. Regular pattern formation in real ecosystems. *Trends in Ecology & Evolution*, 23(3):169–175, March 2008.

[18] E. Gilad, J. von Hardenberg, A. Provenzale, M. Shachak, and E. Meron. A mathematical model of plants as ecosystem engineers. *Journal of Theoretical Biology*, 244(4):680–691, February 2007.

[19] Ehud Meron. Pattern-formation approach to modelling spatially extended ecosystems. *Ecological Modelling*, 234:70–82, June 2012.

[20] Nicolas Barbier, Pierre Couteron, Jean Lejoly, Vincent Deblauwe, and Olivier Lejeune. Self-organized vegetation patterning as a fingerprint of climate and human impact on ssemi-arid ecosystems. *Journal of Ecology*, 94(3):537–547, April 2006.

[21] Stephan Getzin, Hezi Yizhaq, Bronwyn Bell, Todd E. Erickson, Anthony C. Postle, Itzhak Katra, Omer Tzuk, Yuval R. Zelnik, Kerstin Wiegand, Thorsten Wiegand, and Ehud Meron. Discovery of fairy circles in australia supports self-organization theory. *Proceedings of the National Academy of Sciences*, 113(13):3551–3556, March 2016.

[22] CM Duarte. Temporal biomass variability and production/biomass relationships of seagrass communities. *Marine Ecology Progress Series*, 51:269–276, 1989.

[23] Olga Invers, Javier Romero, and Marta Pérez. Effects of pH on seagrass photosynthesis: a laboratory and field assessment. *Aquatic Botany*, 59(3-4):185–194, December 1997.

[24] Mark S. Fonseca, M.A.R. Koehl, and Blaine S. Kopp. Biomechanical factors contributing to self-organization in seagrass landscapes. *Journal of Experimental Marine Biology and Ecology*, 340(2):227–246, January 2007.

[25] Daniel Ruiz-Reynés, Francesca Schönsberg, Emilio Hernández-García, and Damià Gomila. General model for vegetation patterns including rhizome growth. *Physical Review Research*, 2(2), June 2020.

[26] Tomàs Sintes, Núria Marbà, Carlos M. Duarte, and Gary A. Kendrick. Nonlinear processes in seagrass colonisation explained by simple clonal growth rules. *Oikos*, 108(1):165–175, January 2005.

[27] Tomàs Sintes, Núria Marbà, and Carlos M. Duarte. Modeling nonlinear seagrass clonal growth: Assessing the efficiency of space occupation across the seagrass flora. *Estuaries and Coasts*, 29(1):72–80, February 2006.

[28] Daniel Ruiz-Reynés, Damià Gomila, Tomàs Sintes, Emilio Hernández-García, Núria Marbà, and Carlos M. Duarte. Fairy circle landscapes under the sea. *Science Advances*, 3(8), August 2017.

[29] Daniel Ruiz-Reynés. *Dynamics of Posidonia Oceanica Meadows*. PhD thesis, IFISC, 2019.

[30] Juan M. Ruíz, Lazaro Marín-Guirao, and Jose M. Sandoval-Gil. Responses of the mediterranean seagrass posidonia oceanica to in situ simulated salinity increase. *Botanica Marina*, 52(5), January 2009.

[31] Max Rietkerk, Robbin Bastiaansen, Swarnendu Banerjee, Johan van de Koppel, Mara Baudena, and Arjen Doelman. Evasion of tipping in complex systems through spatial pattern formation. *Science*, 374(6564), October 2021.

[32] Fundación Cleanwave. Medgardens. `cleanwavefoundation.org/ca/proyectos/medgardens/`.

[33] Save the Med Foundation. `savethemed.org/es/`.